Research Square

Preprints are preliminary reports that have not undergone peer review.
They should not be considered conclusive, used to inform clinical practice,
or referenced by the media as validated information.

Translational Evaluation of an Intelligent Bipolar Electrosurgical System with Integrated Neurostimulation for IONM

Liang Chen

Chenliang_apllo@163.com

Nanjing University of Posts and Telecommunications

Liang Dai

Peking University Cancer Hospital

Rongqing Xu

Nanjing University of Posts and Telecommunications

Huizhao Gao

Beneeon (Jiangsu) Medical Technology Co., Ltd

Yueqiao Wang

Beneeon (Jiangsu) Medical Technology Co., Ltd

Jiaxue Qi

Beneeon (Jiangsu) Medical Technology Co., Ltd

Article

Keywords: Robot-assisted surgery, Multifunctional surgical instruments, Intraoperative nerve detection, Bipolar coagulation, Energy safety

Posted Date: November 17th, 2026

DOI: https://doi.org/10.21203/rs.3.rs-11013958/v1

License: This work is licensed under a Creative Commons Attribution 4.0 International License.
Read Full License

Additional Declarations: No competing interests reported.

Translational Evaluation of an Intelligent Bipolar Electrosurgical System with Integrated Neurostimulation for IONM

Liang Chen[1*], Liang Dai[2], Rongqing Xu[1], Huizhao Gao[3], Yueqiao Wang[3], Jiaxue Qi[3]

[1]College of Electronic and Optical Engineering, Nanjing University of Posts and Telecommunications, Nanjing 210046, China

[2]Peking University Cancer Hospital, Beijing 100142, China

[3]Beneeon (Jiangsu) Medical Technology Co., Ltd, Taizhou 225300, China

Abstracts

Background: Frequent manual instrument exchanges between bipolar coagulators and neural probes compromise surgical workflow and elevate iatrogenic nerve injury risks. Especially, in robot-assisted surgery, the lack of an auxiliary robotic arm to hold dedicated probes further precludes real-time neural mapping. Consequently, integrating both electrocoagulation and neural stimulation into a single, unified instrument tip addresses an urgent clinical need to enable seamless intraoperative neuromonitoring without sacrificing surgical dexterity.

Methods: This comparative study engineered a parallel-connected isolation transformer topology (E-VTMS) for autonomous electrocoagulation-neurostimulation switching. In vitro efficiency testing (5–70 W) was followed by in vivo signal fidelity and thermal safety evaluations, comparing E-VTMS-driven forceps against gold-standard commercial probes in rodent sciatic and porcine recurrent laryngeal nerve models. Electrophysiological non-inferiority was quantified via paired t-tests.

Results: In vitro testing demonstrated >98% energy efficiency (4.4 W vs. 4.5 W at 5 W baseline, 69.2 W vs 69.8W at 70W baseline). In vivo trials confirmed diagnostic non-inferiority, eliciting neural signals indistinguishable from gold-standard commercial probes (paired t-test; sciatic nerve: $P = 0.286$; recurrent laryngeal nerve: $P = 0.806$). Post-30W activation, saline irrigation and tissue contact rapidly cooled tips below the 42°C neural threshold (decay rates: 37.25°C/s and 11.56°C/s). Combined with 0 mA open-circuit leakage, these boundaries eliminate iatrogenic injury.

Conclusions: The E-VTMS platform integrates clinical IONM and electrosurgery into a single shared bipolar end-effector. This automated bimodal design eliminates manual instrument exchanges, optimizing surgical workflow and mitigating iatrogenic risks. Rigorously validated for thermal safety and electrophysiological fidelity, the technology demonstrates robust readiness for human clinical translation.

Keywords: Robot-assisted surgery; Multifunctional surgical instruments; Intraoperative nerve detection; Bipolar coagulation; Energy safety

Funding: This work was supported by the Jiangsu Provincial Special Fundfor Science and Technology (Grant No.BE2023762);

***Corresponding author:**Liang Chen;

Email:chenliang_appllo@163.com;

Ethics approval: All animal experiments were approved by the Institutional Animal Care and Use Committee (IACUC) [Approval No. IACUC24-0138]. The experiments were conducted in accordance with the Chinese National Standard Guidelines for the Ethical Review of Animal Welfare (GB/T 35892-2018). Furthermore, this study is reported in accordance with the ARRIVE guidelines.

1. Introduction

1.1 Clinical Background and Technological Limitations

Intraoperative neuromonitoring (IONM) and bipolar electrocoagulation are concurrent essentials in delicate surgical disciplines for preserving neural integrity and achieving precise hemostasis. Conventionally, these modalities require standalone instruments. Prior integration attempts via mechanical switches [1] or foot pedals [2] reduce instrument exchange times but still rely on manual intervention. In microsurgery, this lack of automation forces surgeons to divert their visual attention from the operating microscope (Fig. 1) to physically swap instruments [3, 4]. This repetitive exchange disrupts surgical workflows, prolongs operative time, and elevates iatrogenic risks to adjacent eloquent tissues [5].

This operational bottleneck is further exacerbated in robot-assisted surgery. While robotic systems deliver superior dexterity and tremor filtration for precise dissection, typical platforms operate with a constrained number of robotic arms, and port-placement configurations restrict the concurrent introduction of multiple instruments. Because the available end-effectors are predominantly monopolized by essential surgical tools such as bipolar graspers and scissors, dedicated neural probes cannot be simultaneously accommodated. Surgeons are therefore forced either to endure cumbersome, repetitive tool exchanges through the robotic trocars or to forego continuous neuromonitoring altogether during critical dissection phases, thereby severely undermining surgical efficiency and patient safety[6].

To achieve full automation, recent bioengineering efforts have explored circuit-level bimodal integration. A primary literature approach utilizes conventional Current Transformer Monitoring Systems (CTMS) for state sensing. However, traditional

CTMS topologies fail to block high-voltage transient surges during electrosurgical unit (ESU) activation, causing hazardous current leakage that can catastrophically damage downstream neurostimulation modules and compromise neural safety. Although enhanced iterations (E-CTMS) attempted to mitigate these risks, their series-connected sensing paths remain incapable of reliably detecting weak electrocoagulation outputs at delicate micro-surgical thresholds (e.g., 5 W) while introducing unacceptable insertion losses (>10%) that heavily degrade clinical coagulation efficiency.

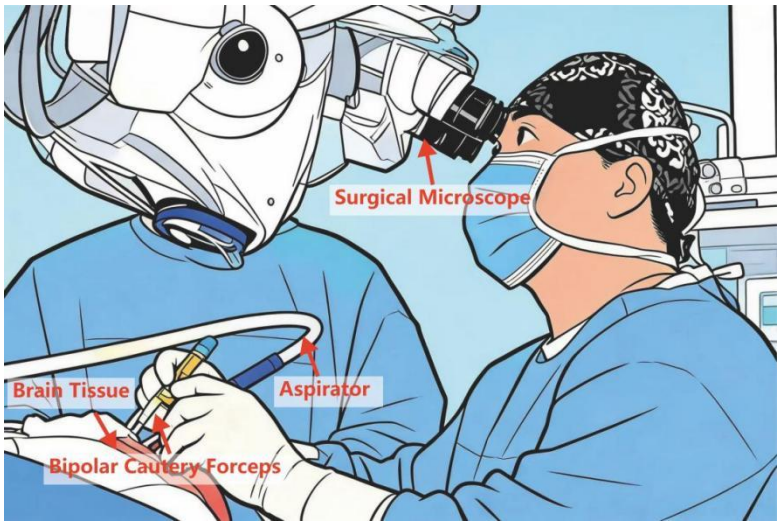


Fig.1 Schematic Illustration of Bipolar Coagulation in Neurosurgery

1.2 Proposed Solution and Translational Significance

Consequently, existing bimodal frameworks cannot simultaneously achieve high-sensitivity detection, low insertion loss, and absolute electrical safety. To address this critical gap and offer a necessary contribution to the field, this study introduces the E-VTMS platform. By employing a parallel-connected isolation transformer topology with direct magnetic coupling, the proposed architecture successfully decouples the historical trade-offs between hardware safety and sensing

fidelity. The specific aims of this study are to systematically evaluate the energy transmission efficiency of the E-VTMS in vitro, and to rigorously validate its electrophysiological signal fidelity and thermal safety in vivo using rodent and porcine models.

The translational significance of the E-VTMS is threefold. First, it features universal plug-and-play compatibility, seamlessly interfacing with standard hospital IONM and ESU equipment without requiring wholesale replacement. Second, it holds transformative potential for robotic-assisted surgeries (e.g., the da Vinci Surgical System). By integrating this intelligent controller, standard robotic instruments (such as Maryland forceps) can be retrofitted to automatically deliver both precise coagulation and neural probing. Ultimately, by definitively eliminating manual instrument exchanges, mitigating iatrogenic nerve injury, and optimizing operative efficiency, this platform represents a rigorously validated technology highly ready for human clinical translation.

2. System Design and Architecture

2.1 System Requirements and Design Criteria

To achieve a clinically viable and inherently safe bimodal integration of the electrosurgical unit (ESU) and intraoperative neuromonitoring (IONM), an ideal hardware architecture must satisfy four stringent operational criteria. These requirements ensure both structural reliability across a wide dynamic power range and paramount patient safety:

1. Reliable Actuation and Protection Across a Wide Dynamic Power Range: The robust detection circuitry must guarantee effective electrocoagulation output across a broad ESU power spectrum (5 W to 70 W). ¬This necessitates a dual hardware capability: exceptional sensitivity to ensure instantaneous threshold triggering during low-power delicate tissue dissection (5 W), seamlessly combined with robust

overvoltage and overcurrent protection to sustain continuous high-energy surges (up to 70 W) without circuit degradation.

2. Maximal Energy Transmission Efficiency: Regardless of the active power configuration (low or high), the system must minimize energy insertion loss. The system must maintain a power transmission efficiency of at least 90% relative to a conventional, unmediated hardware connection. This strictly preserves the intrinsic thermal cutting and coagulation efficacy of the clinical bipolar forceps.

3. Absolute Prevention of Electrical Energy Leakage: During autonomous bimodal transitions, the system must strictly eliminate any hazardous high-frequency energy leakage. The ultimate clinical priority of this fail-safe mechanism is to fundamentally preclude irreversible neural damage caused by stray currents. Concurrently, this design provides the essential hardware benefit of safeguarding the neurostimulator's internal fuse, thereby preventing catastrophic system failure during surgery.

4. Strict Thermal Safety and Minimal Heat Spread: Beyond electrical isolation, the integrated system must optimize energy delivery to prevent excessive heat accumulation at the bipolar instrument tip. The working temperature of the instrument must be strictly maintained below the critical threshold for neural thermal injury (e.g., 42°C) during electrocoagulation. This minimizes lateral thermal spread, fundamentally protecting adjacent sensitive neural structures from direct physical heat damage.

2.2 Overall Composition of the Bimodal Surgical System

The integrated platform bridges a standard intraoperative neuromonitoring (IONM) system and a bipolar electrosurgical unit (ESU) via a proprietary Intelligent Bipolar Controller. Functioning as a bidirectional hub, the controller simultaneously receives low-current stimulation signals from the IONM and high-frequency energy from the ESU. Its unified output channels both modalities directly into standard bipolar forceps. This topological configuration (Fig. 2) effectively transforms a conventional surgical tool into a dual-modality instrument for on-demand neurostimulation or electrocoagulation.

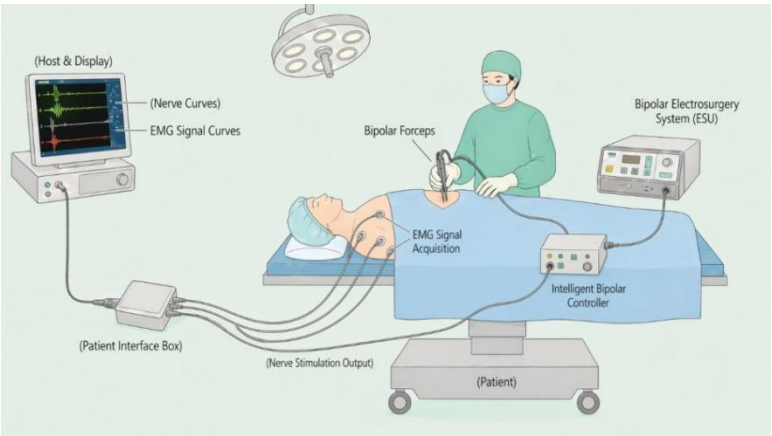


Fig.2 Intraoperative workflow and mechanism of action of the intelligent dual-modality bipolar system

To facilitate autonomous functional transitions (Fig. 3), the controller employs an electromagnetic mutual inductance circuit to continuously monitor ESU activity. The system instantaneously toggles to the coagulation pathway upon detecting a high-frequency surge and inherently defaults back to the neurostimulation state upon cessation. To optimize this rapid switching and ensure robust circuit isolation, three architectural iterations were engineered and systematically evaluated: the Current Transformer Monitoring System (CTMS), the Enhanced CTMS (E-CTMS), and the Enhanced Voltage Transformer Monitoring System (E-VTMS).

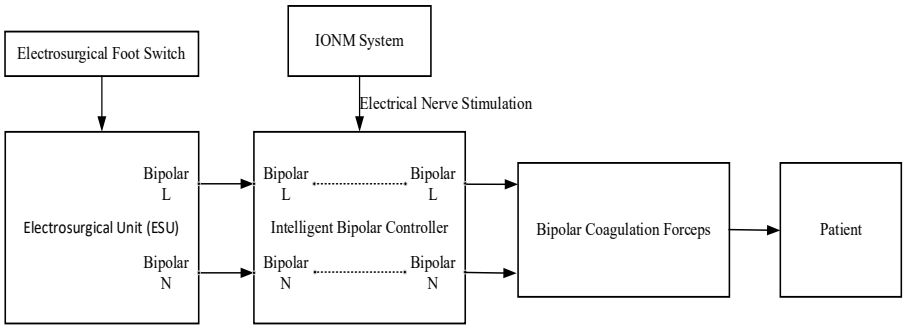


Fig.3 Schematic architecture and signal routing topology of the integrated dual-modality surgical platform

2.3 Evaluation of Bimodal Prototype Topologies

2.3.1 Current Transformer Monitoring System (CTMS)

The baseline CTMS (Fig. 4) employs a mutual inductor circuit to actuate modality-switching relays. However, a transient switching latency between ESU activation and relay isolation permitted catastrophic high-frequency energy backflow into the IONM circuitry, rendering this initial architecture clinically unviable.

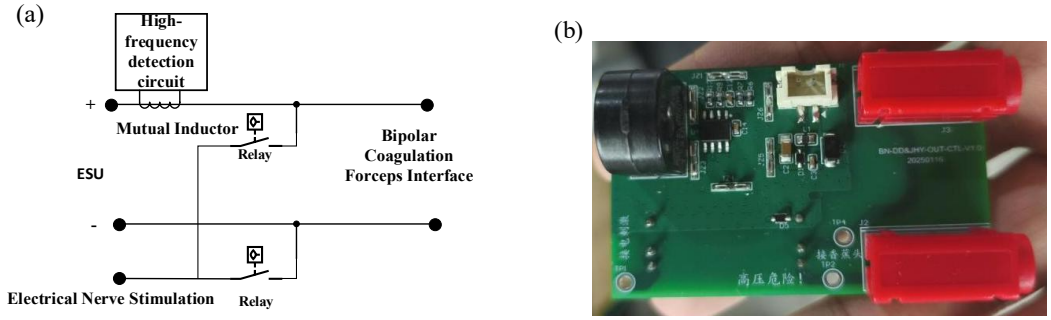


Fig.4 Current Transformer Monitoring System(CTMS).(a)Schematic Diagram of CTDS;(b) PCBA of CTMS

2.3.2 Enhanced Current Transformer Monitoring System (E-CTMS)

To circumvent the latency-induced hardware failure, the E-CTMS(Fig. 5) introduces a low-capacitance load across the ESU output terminals and upgrades the switching architecture to a double-pole double-throw (DPDT) relay . This configuration facilitates the preemptive detection of minute initial currents, allowing the relay to instantaneously actuate the coagulation pathway prior to the primary energy surge. This ensures robust, absolute electrical isolation of the sensitive neurostimulation circuitry.

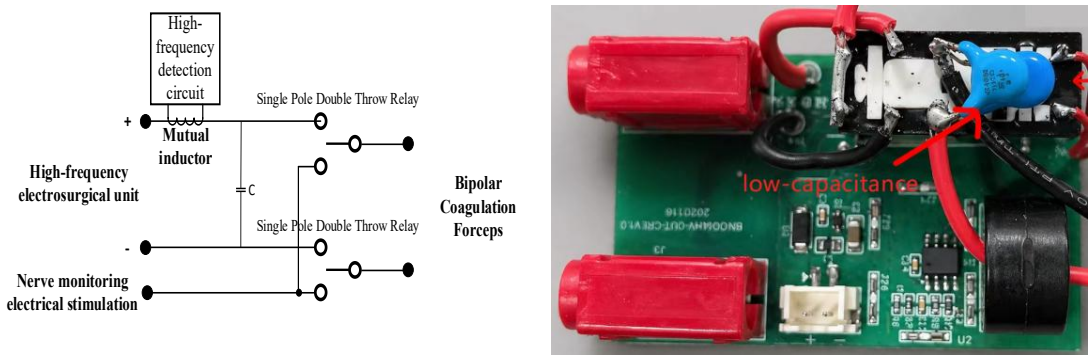
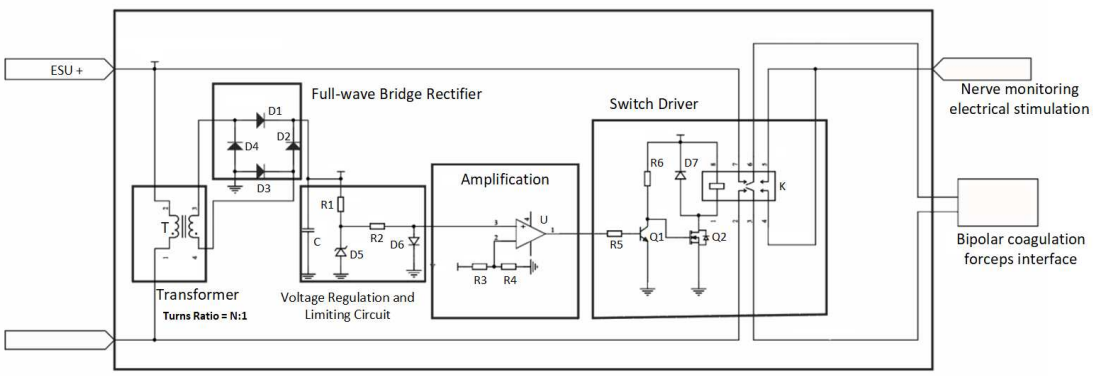


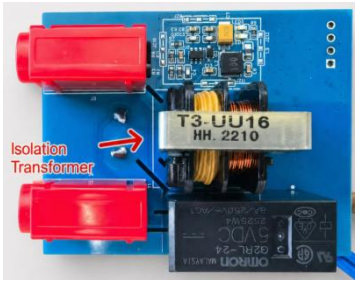
Fig.5 E-CTMS Core.(a)Schematic Diagram of E-CTMS;(b) PCB of E-CTMS

2.3.3 Enhanced Voltage Transformer Monitoring System (E-VTMS)

To address the vulnerabilities of conventional capacitive-coupled configurations, the E-VTMS employs a isolation transformer to establish robust galvanic separation via direct magnetic coupling, inherently shielding the IONM circuitry from electrosurgical (ESU) surges. As depicted in the core hardware schematic (Fig. 6), the bimodal switching logic is governed by the induced high-frequency voltage, which is determined by the transformer's turns ratio and rectification efficiency. Following amplification, this voltage is continuously evaluated against a predefined safety threshold: exceeding it triggers a downstream relay to instantaneously route ESU energy to the output port, whereas sub-threshold signals autonomously default to delivering the IONM stimulation.



(a)Hardware design and implementation circuit of the E-VTMS;



(b) PCB of E-VTMS

Fig.6 Core system design of the E-VTMS

The theoretical calculation for the induced voltage of the high-frequency electrosurgical signal can be expressed as follows:

$$V_{out}=V_{in}\times\frac{1}{N}\times\eta\times\sqrt{2}\times Au$$

Where V_{out} represents the output voltage; V_{in} is the input signal; N represents the turns ratio of the transformer, and η represents the rectification coefficient, where 95% is optimally preferred. Au represents the amplification factor of the amplifier.

Future Perspectives: Sensorless Thermal Safety Monitoring

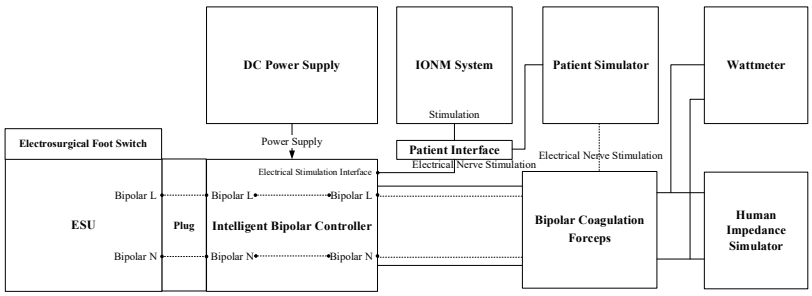
Furthermore, this mathematical model establishes a critical foundation for advanced thermal management. In future iterations, this formula can be utilized to calculate the real-time power output of the electrosurgical unit. By integrating the actuation time and real-time power, the cumulative thermal energy generated at the distal tip of the bipolar forceps can be accurately quantified. This methodology allows for the predictive assessment of the tip's thermal safety without the necessity of embedding physical temperature sensors at the surgical site. Consequently, this "sensorless" thermal monitoring strategy will significantly reduce hardware complexity and ensure seamless plug-and-play adaptability with existing clinical electrosurgical systems.

3. System Performance Evaluation

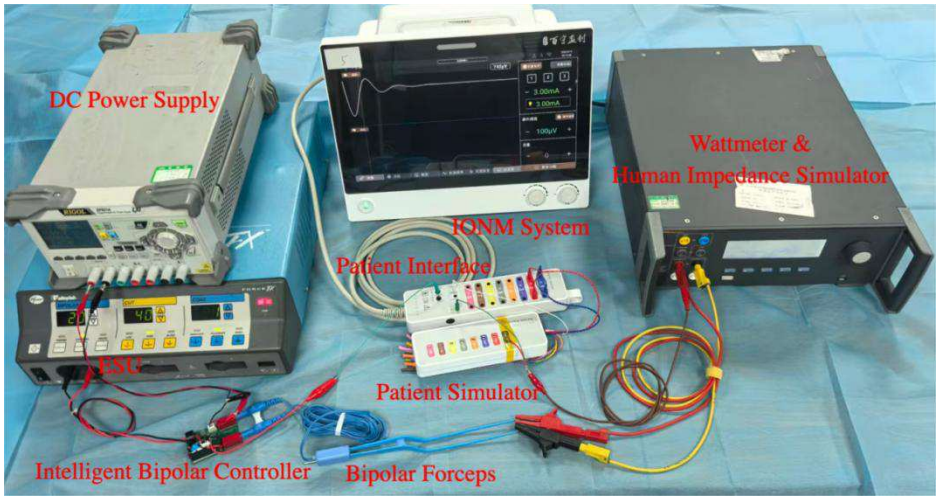
3.1 In Vitro Bench Testing Architecture

An in vitro platform (Fig. 7) was engineered to evaluate the proposed bimodal controller, comprising a commercial IONM system (BN-JCY-280; Beneeon, Taizhou, China) and an electrosurgical unit (FX-8; Valleylab, Boulder, CO, USA).To validate each modality systematically, the Bipolar Coagulation Forceps (BN-D-A1-180-1.0-4WS; Beneeon, Taizhou, China) was independently coupled to two distinct modules: a tissue impedance simulator equipped with a high-precision wattmeter (QA-ES III; Fluke Biomedical, Everett, WA, US) to quantify ESU energy, and a neural patient simulator (BN-JCY-282; Beneeon, Taizhou, China) to verify IONM-evoked electromyographic (EMG) responses.

Operational Logic: Actuating the ESU foot-pedal instantly routes high-frequency energy to the impedance simulator for power evaluation. Upon release, the controller autonomously defaults to neurostimulation. Low-current pulses are delivered to the patient simulator, eliciting synthetic EMG responses immediately captured by the IONM interface, thereby confirming the system's bidirectional closed-loop efficacy.



(a) Block diagram for bimodal mechanism evaluation



(b) Experimental setup

Fig 7. *In vitro* bench testing architecture.(a)Block diagram for bimodal mechanism evaluation. (b) Experimental setup. The ESU and IONM systems are integrated via the Intelligent Bipolar Controller to validate neuro-monitoring functionality and electrocoagulation power output.

3.2 Bipolar Coagulation Performance and Mechanistic Analysis

Energy delivery efficiency was benchmarked across three configurations (Direct Connection Style [DCS, baseline], E-CTMS, and E-VTMS) utilizing a 100 Ω impedance load (Fig. 8). At a 70 W high-power setting, the E-VTMS demonstrated >99% transmission efficiency, achieving near-perfect equivalence with the DCS baseline (Pearson's $r > 0.999$). Conversely, the E-CTMS exhibited significant attenuation (yielding only 90% of baseline output) because its intrinsic load capacitor introduced parasitic capacitive reactance, inherently dissipating tissue-directed energy.

Crucially, at a delicate 5 W micro-surgical setting, the sub-threshold current traversing the E-CTMS capacitor failed to trigger the high-frequency detection relay, resulting in complete actuation failure. By exclusively leveraging direct magnetic transformer coupling, the E-VTMS eliminates these parasitic impedances, preserving maximal transmission fidelity across all power gradients.

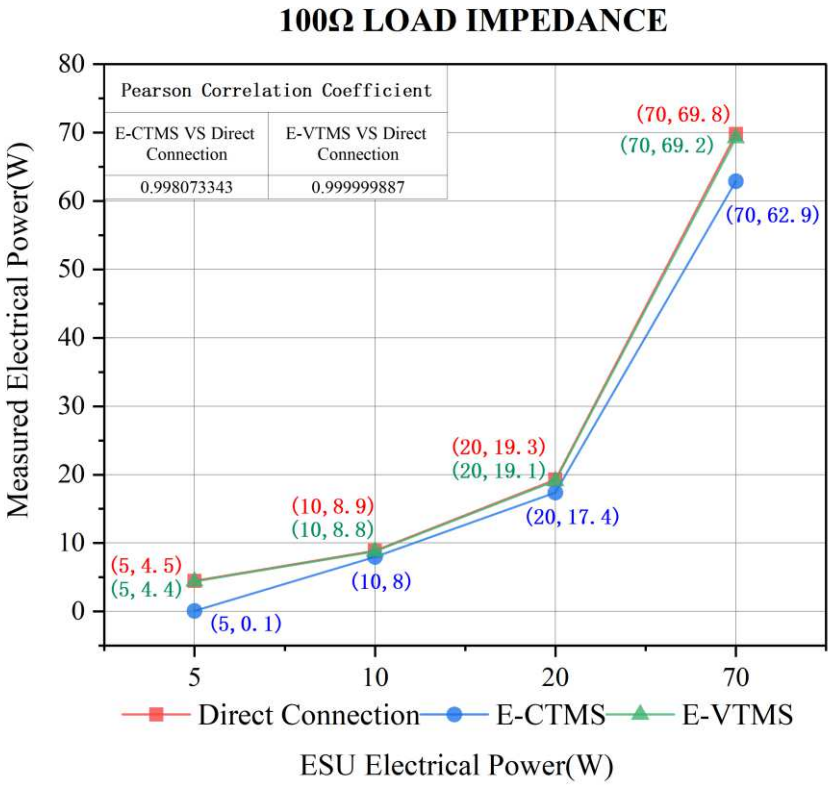


Fig.8 Comparative power output profiles of the DCS, E-CTMS, and E-VTMS architectures under standardized impedance.

In summary, comprehensive in vitro bench evaluations definitively validate that the E-VTMS architecture overcomes the fundamental energy attenuation and low-power actuation failures inherent to capacitive-coupled designs. By guaranteeing >99% power transmission fidelity while maintaining absolute physical isolation, the system fulfills all electro-physical prerequisites for safe bimodal operation. This robust hardware foundation directly justifies and prompts the subsequent in vivo translational validations to assess its clinical neuroprotective efficacy.

4. In Vivo Preclinical Validation and Thermal Safety Assessment

Neural tissue incurs irreversible damage exceeding 42°C, whereas non-neural soft tissues tolerate thresholds up to 60°C [7-12]. Consequently, quantifying the thermal dynamics and electrophysiological fidelity of the integrated forceps is imperative to preclude iatrogenic neural injury during automated bimodal transitions.

4.1 Small Animal Model: Rat Sciatic Nerve Evaluations

4.1.1 In Vivo Platform Architecture

To validate system efficacy and thermal safety, an *in vivo* rat sciatic nerve model was established (**Fig. 9**). The experimental architecture seamlessly integrated the standard ESU and IONM consoles via the E-VTMS controller. Crucially, the dual-modality bipolar forceps were custom-retrofitted with a micro-thermocouple sensor. Paired with a high-precision thermometer and subdermal needle electrodes, this configuration enabled real-time, highly granular thermal monitoring during fully automated transitions between high-frequency coagulation and neurostimulation.

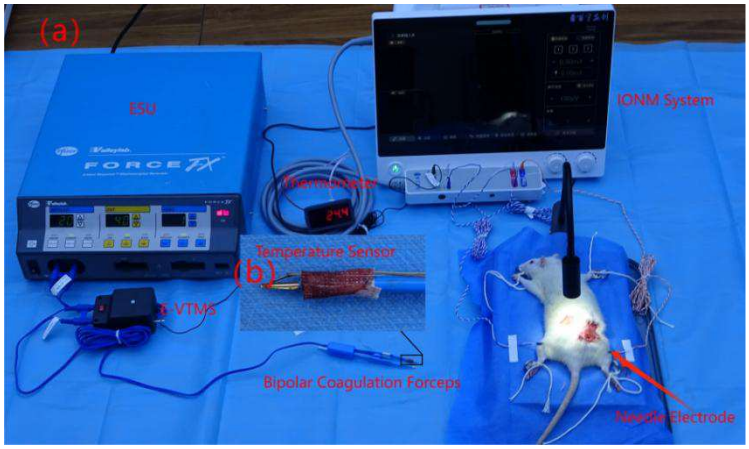


Fig 9. In vivo experimental architecture for the rat sciatic nerve model. (a) Macroscopic view of the surgical environment integrating the E-VTMS dual-modality platform. (b) Magnified view of the

bipolar coagulation forceps, custom-integrated with a micro-thermocouple sensor for real-time thermal dynamic profiling at the tissue interface.

4.1.2 Thermal Dissipation Dynamics and Cooling Modality Optimization

To mitigate lateral thermal spread post-activation (30 W), the thermal dissipation dynamics of three cooling modalities were quantified(Fig. 10). Active saline irrigation demonstrated optimal efficacy, capping peak tip temperature at 67.8°C with a maximal decay rate of 37.25°C/s. Immediate thermal transfer via adjacent tissue contact also effectively reduced temperatures below the critical 42°C neural threshold within 3 seconds (11.56°C/s). Ambient air cooling, conversely, proved clinically inadequate (6.32°C/s). Mechanistically, synergizing these active cooling protocols with short-burst high-frequency activation facilitates inter-pulse thermal relaxation, rigorously restricting the thermal injury radius and preserving delicate neurovascular structures.

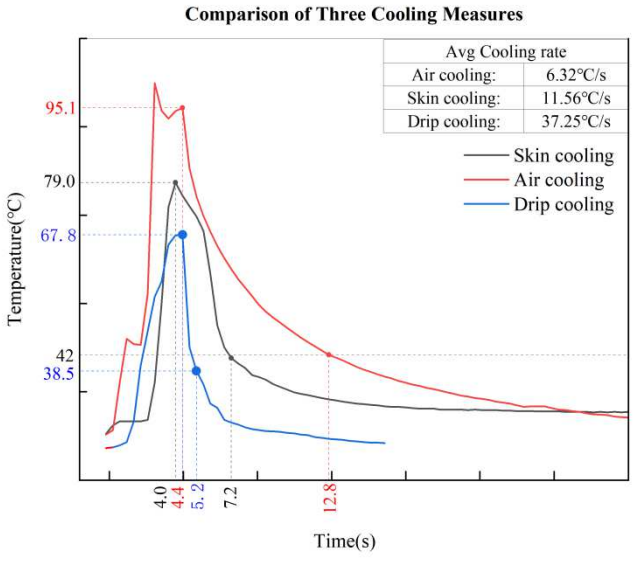


Fig 10. Comparative thermal dissipation dynamics across active and passive cooling modalities.

The temperature decay profiles following a 30 W bipolar activation illustrate the efficacy of active

saline irrigation (drip) and adjacent tissue contact (skin) in rapidly dissipating tip temperatures below the critical 42°C threshold, contrasting with the inadequate cooling rate of ambient air.

4.1.3 Comparative Electrophysiological Efficacy in Sciatic Nerve (SN) Monitoring

The in vivo(Fig.11) stimulation efficacy of the integrated bimodal forceps was evaluated against a standard commercial neural probe on the sciatic nerves of adult male Sprague-Dawley rats (aged 6–8 weeks, weighing 220–250 g) across incremental stimulus intensities (0.5–1.5 mA).As detailed in Table 1, the elicited compound muscle action potential (CMAP) amplitudes demonstrated high concordance between the two modalities. A paired t-test confirmed no statistically significant difference in physiological impact (paired t-test, $P = 0.286$). This validates that the dual-function forceps maintain signal fidelity equivalent to dedicated commercial probes in a small animal model.

Table 1 Comparative CMAP amplitudes elicited by the integrated bipolar forceps and a standard neural probe across ascending stimulation currents

Stimulation Current (mA)	Integrated Bipolar Forceps (μV)	Standard Neural Probe (μV)
0.5	1211	1174
1	1308	1505
1.5	1460	1609



Fig 11. Intraoperative neurostimulation modalities for functional nerve assessment. (a) Conventional probing executed with a standard neural probe. (b) Bimodal probing executed with the intelligent bipolar electrocautery forceps, maintaining high signal fidelity.

4.2 In Vivo Porcine Thyroid Model: Electrophysiological Mapping of the Recurrent Laryngeal (RLN) and Vagus (VN)Nerves

To definitively establish translational applicability, the electrophysiological fidelity of the integrated platform was quantified in an in vivo porcine thyroid model (Fig.12) utilizing Yorkshire minipigs (4–6 months old, weighing 20–30 kg), targeting the highly vulnerable recurrent laryngeal nerve (RLN) and vagus nerve across clinically relevant stimulation thresholds (1.0–3.0 mA) (Table 2).

For the RLN, CMAP amplitudes evoked by the dual-modality forceps demonstrated absolute statistical equivalence to the standard neural probe (paired t-test, $P = 0.806$). Notably, while vagus nerve recordings yielded a marginal statistical variance (paired t-test, $P = 0.026$), the maximal absolute amplitude divergence was strictly confined to <3% (e.g., 1023 μV vs. 1053 μV at 3.0 mA). Neurophysiologically, this micro-variance is clinically negligible. Consequently, these robust quantitative metrics definitively validate that the integrated end-effector delivers non-inferior, high-fidelity neuromonitoring during complex thyroid dissections without compromising intrinsic neural electrophysiology (Fig. 13).

Table 2. Comparative CMAP amplitudes of RLN and vagus nerves elicited by the integrated bipolar forceps versus a standard neural probe

Stimulation Current (mA)	RLN (μV)		Vagus Nerve (μV)	
	Integrated Forceps	Neural Probe	Integrated Forceps	Neural Probe
1.0	1211	1168	979	1001
2.0	1308	1328	1021	1038
3.0	1460	1505	1023	1053



Fig 12. Comparative intraoperative neuromonitoring during complex cervical dissection. (a) Baseline signal elicitation utilizing a dedicated neural probe. (b) Seamless bimodal neural probing executed with the intelligent electrocautery forceps, preserving structural integrity without instrument exchange.



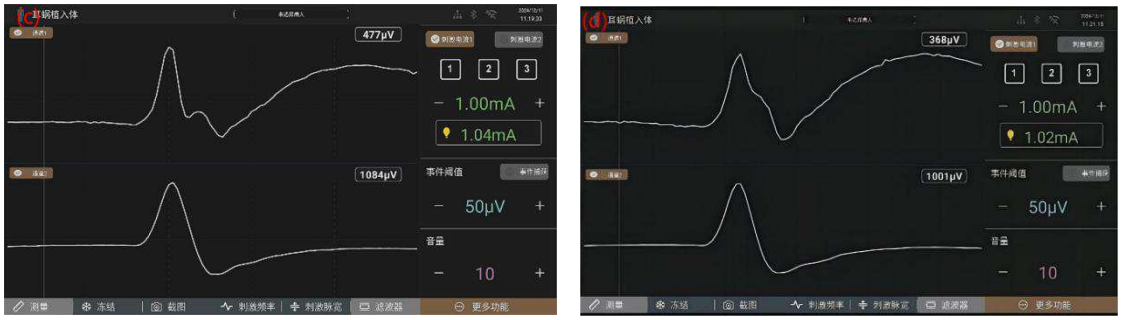


Fig 13. Representative electromyographic (EMG) waveforms demonstrating high signal fidelity in the porcine thyroid model. (a, b) Compound muscle action potentials (CMAPs) of the recurrent laryngeal nerve (RLN) elicited by the standard dedicated neural probe (baseline control) and the proposed integrated bipolar forceps, respectively. (c, d) Corresponding CMAP traces for the vagus nerve (VN) elicited by the standard probe and the integrated forceps. Note the exceptional morphological and quantitative concordance between the two modalities, confirming that the integrated architecture introduces no electrophysiological distortion.

4.3 Fail-Safe Efficacy Against Inadvertent ESU Actuation on the Porcine Recurrent Laryngeal Nerve

To validate the system's protective capacity against critical surgical deviations, a simulated inadvertent ESU actuation was executed during active RLN mapping. Mechanistically, precise neuro-probing necessitates an unapproximated forceps configuration, utilizing a single tip as a focal stimulating electrode. This topography inherently establishes an absolute open-circuit for bipolar high-frequency energy (Table 3). Consequently, deliberate foot-pedal depression during this phase physically precludes circuit completion and subsequent energy emission. This intrinsic hardware-level fail-safe guarantees zero iatrogenic electrical trauma to the neural structure, definitively neutralizing the risk of user-error-induced morbidity.

Table 3. Quantitative validation of the intrinsic fail-safe mechanism during simulated inadvertent ESU actuation on the porcine recurrent laryngeal nerve.

Anatomical Site	Standard Neural Probe (μV)	Integrated Bipolar Forceps: Normal Probing (μV)	Integrated Bipolar Forceps: Inadvertent Actuation (μV)
Site 1	719	754	749
Site 2	758	768	728

5. Discussion

The E-VTMS successfully achieves automated bimodal ESU-IONM integration, optimizing surgical workflows and eliminating iatrogenic risks associated with manual instrument swapping. When evaluated in the context of existing literature, the architectural superiorities of this parallel-connected isolation transformer topology become distinct. Prior bimodal connection schemes predominantly relied on conventional Current Transformer Monitoring Systems (CTMS). However, circuit evaluations reveal that traditional CTMS topologies fail to block high-voltage transient surges, leading to hazardous current leakage that can catastrophically damage the downstream neurostimulation module and compromise neural safety. Although subsequent enhanced iterations (E-CTMS) attempted to address these risks, their series-connected sensing paths remain fundamentally incapable of reliably detecting weak electrocoagulation outputs at micro-surgical thresholds (e.g., 5 W), while introducing unacceptable insertion losses (>10%) that heavily degrade standard coagulation efficiency. In contrast, the proposed E-VTMS leverages direct magnetic coupling to establish robust galvanic separation, successfully sustaining a power transmission efficiency exceeding 98% across the full dynamic range (5 W to 70 W) while ensuring absolute hardware and neural safety.

From a physiological perspective, in vivo validations demonstrated complete

diagnostic non-inferiority, yielding CMAP amplitudes statistically equivalent to gold-standard commercial probes (paired t-test, SN, P = 0.286;RLN, P =806). This confirms that the parallel isolation circuitry preserves signal fidelity without attenuating the micro-current pulses required for precise nerve mapping. Furthermore, thermal evaluations highlight a robust, dual-layer fail-safe boundary: the hardware-level open-circuit configuration during the probing phase strictly restricts high-frequency leakage to 0 mA, while incorporating standard intraoperative cooling methods (saline irrigation or tissue contact) effectively dissipates latent heat, rapidly confining the working tip temperature below the 42°C critical threshold for neural thermal injury.

Limitations and Future Work

Despite these validated profiles, certain limitations exist. First, current in vivo trials were restricted to acute surgical windows; long-term functional recovery must be verified in chronic survival models. Second, the system currently lacks an active temperature feedback loop, relying on passive clinical cooling to manage thermal risks. To transition from passive safety to intelligent closed-loop protection, our future developmental roadmap includes integrating ultra-miniature thermocouple temperature sensors and dedicated thermal data acquisition modules directly onto the bipolar end-effector tips. This hardware iteration will enable real-time tracking of the exact instrument temperature, empowering the microcontroller unit to dynamically modulate or interrupt ESU energy delivery the instant a critical biological thermal boundary is breached.

6. Conclusions

The E-VTMS establishes an automated, bimodal surgical platform that achieves

seamless transitions between bipolar electrocoagulation and intraoperative neuromonitoring through a single shared end-effector. By deploying a parallel magnetic-coupling topology, the system decouples the historical trade-offs of series current-sensing frameworks, sustaining an energy transmission efficiency exceeding 98% while providing absolute galvanic separation. In vivo evaluations robustly validate its dual-layer fail-safe boundaries, strictly restricting high-frequency leakage to 0 mA and reliably confining the instrument tip temperature below the 42°C critical neurological threshold. Furthermore, the platform demonstrates complete diagnostic non-inferiority, yielding electrophysiological mappings statistically equivalent to dedicated gold-standard commercial probes. Ultimately, by eliminating manual instrument exchanges, the E-VTMS optimizes surgical workflows and maximizes patient safety, representing a rigorously validated technology highly ready for human clinical translation.

References

[1] Ferlay J, Soerjomataram I,Dikshit R, et al. Cancer incidence and mortality worldwide: sources, methods and major patterns in GLOBOCAN 2012[J]. International Journal of Cancer, 2015, 136(5): E359-E386.

[2] Sitges-Serra A, Ruiz S, Girvent M, et al.Outcome of protracted hypoparathyroidism after total thyroidectomy[J]. British Journal of Surgery, 2010, 97(11): 1687-1695.

[3] Eivazi S, Afkari H, Bednarik R,et al. Analysis of disruptive events and precarious situations caused by interaction with neurosurgical microscope[J]. Acta Neurochir (Wien). 2015;157(8):1413-1420.

[4] .Mukash, Gaukhar, et al.Evaluation of visual ergonomics in microsurgery: a real-time video processing solution[J]. Acta Neurochirurgica 167.1 (2025): 1-13.

[5] Stopa M, Barczyński M. Current knowledge on the use of neuromonitoring in thyroid surgery[J]. Medicina (Kaunas). 2024;60(3):675.

[6] Materazzi, Gabriele, and Leonardo Rossi. Robotic Surgery and IONM[J].Neuromonitoring in Thyroid and Parotid Surgery: A Practical Guide. Cham: Springer Nature Switzerland, 2025. 121-128.

[7] Yarmolenko PS, Moon EJ, Landon C, et al. Thresholds for thermal damage to normal tissues: an update[J]. Int J Hyperthermia. 2011;27(4):320-343.

[8] Siracusano S, Daffara C, Muradore R, Marchioro G. Measuring thermal spread during bipolar cauterizing using an experimental pneumoperitoneum and thermal sensors[J]. Front Surg. 2023;10:1115570.

[9] El-Sayed A. Principles and safe use of electrosurgery in minimally invasive surgery[J]. Ann Laparosc Endosc Surg. 2021;6:25.

[10] Koninckx PR, Ussia A, Amro B, et al. Electrosurgery: heating, sparking and electrical arcs[J]. Facts Views Vis Obgyn. 2024;16(3):281-290.

[11] Dodde RE, Bull JL, Shih AJ. Bioheat transfer and thermal damage in electrosurgical vessel sealing. Ann Biomed Eng[J]. 2012;40(12):2626-2638.

[12] Massarweh NN, Cosgriff N, Slakey DP. Electrosurgery: history, principles, and current and future uses. J Am Coll Surg[J]. 2006;202(3):520-530.

Declarations

Competing interests: The authors declare that they have no competing interests.

Ethics approval: All animal experiments were approved by the Institutional Animal Care and Use Committee (IACUC) [Approval No. IACUC24-0138]. The experiments were conducted in accordance with the Chinese National Standard Guidelines for the Ethical Review of Animal Welfare (GB/T 35892-2018). Furthermore, this study is reported in accordance with the ARRIVE guidelines.

The animal experiments in this study were commissioned by company (Beneeon (Jiangsu) Medical Technology Co., Ltd) and executed by Jiangsu Kerbio Medical Technology Group Co., Ltd., a qualified Contract Research Organization (CRO) with certified animal testing facilities and an established Institutional Animal Care and Use Committee (IACUC).

Because all animal housing, handling, and surgical procedures were physically performed at Jiangsu Kerbio's animal facilities, the study protocol was formally submitted to, reviewed, and approved by the IACUC of Jiangsu Kerbio Medical Technology Group Co., Ltd under Approval No. IACUC24-0138.

Availability of data and materials: The datasets generated and analysed during the current study are not publicly available due to intellectual property considerations regarding the proprietary hardware design, but are available from the corresponding author on reasonable request.

Adherence to national and international guidelines: All methods were carried out in accordance with relevant guidelines and regulations.

Consent for publication: Not applicable.

Funding: This work was supported by the Jiangsu Provincial Special Fund for Science and Technology (Grant No. BE2023762).

Email:chenliang_appllo@163.com;

dailiangsharp26@bjmu.edu.cn;

xurq@njupt.edu.cn;

yf-yj-2@bnycmed.com;

wyq@bnycmed.com;

xue@bnycmed.com;

Author Contributions

Liang Chen: Conceptualization, Methodology, Investigation, Writing – original draft.

Liang Dai: Clinical investigation, Supervision, Writing – review & editing.

Rongqing Xu: Supervision, Methodology, Writing – review & editing.

Huizhao Gao: Resources (Hardware PCB design), Methodology.

Yueqiao Wang: Software, Methodology.

Jiaxue Qi: Investigation (Animal experiments).

Euthanasia Protocol:

At the conclusion of the electrophysiological and thermal safety evaluations, all animals were humanely euthanized while under deep anesthesia, adhering strictly to the AVMA Guidelines for the Euthanasia of Animals.

For rats : Rats were deeply anesthetized with 3%–5% isoflurane via inhalation until fully unresponsive to noxious stimuli (pedal withdrawal reflex absent). Euthanasia was then performed by cervical dislocation. Death was verified by checking for respiratory and cardiac arrest.

For swine : While maintained under surgical anesthesia (2.0%–3.0% isoflurane), euthanasia was induced via rapid intravenous injection of potassium chloride (KCl, 1–2 meq/kg) via the marginal ear vein. Death was confirmed by continuous electrocardiographic (ECG) monitoring demonstrating irreversible cardiac arrest, absence of corneal reflex, and permanent cessation of spontaneous respiration.